やすい．これはしばしば両側性である．画像診断としてはMRI，特に矢状断が必須であり，T1強調画像では比較的低信号域，T2強調画像では高信号域で，橋の腫大を示す(図)．ガドリニウムによる増強効果は示さないことも多く，また増強効果がみられたとしても不均一であることが多い．橋病変は延髄には浸潤していないことが多く，これは横走する橋小脳路がバリアーとなっているためとされる．一方中脳や小脳脚方向には初期から浸潤性の進展がみられることが多い．

腫瘍の占拠部位から手術による摘出は通常行われない．従って診断は専ら画像所見によって行われる．剖検のデータではびまん性脳幹部神経膠腫のほとんどは退形成性星細胞腫または膠芽腫であり臨床経過もこれを裏付けている[4]．

表2　びまん性脳幹部神経膠腫に対するhyperfractionation法による放射線照射の臨床試験成績

試験名，照射方法	患者数	生存期間中央値(月)	1年生存率(%)
POG 8495 70.2 Gy in 1.17 Gy fr	131	10	40
POG 9239 70.2 Gy in 1.17 Gy fr＋Cisplatin	130	8	27
CCG 9882 72 Gy in 1 Gy fr	53	9	38
CCG 9882 78 Gy in 1 Gy fr	66	9.5	35

POG：Pediatric Oncology Group，CCG：Children's Cancer Group，fr：fraction

表3　びまん性脳幹部神経膠腫に対する化学療法併用放射線照射の成績

治療内容	患者数	成　績	文献
放射線照射 50-60 Gy CCNU＋VCR＋Prednisone	39	生存期間中央値 9ヵ月 5年生存率 23%	11
放射線照射 70.2 Gy (hyperfractionation) Cisplatin	130	生存期間中央値 8ヵ月 1年生存率 27%	8
放射線照射 54 Gy VP-16＋Trofosfamide	18	1年生存率 27%	12
放射線照射 70.2 Gy (hyperfractionation) VP-16＋Carboplatin	9	8/9例が中央値44週で死亡 1/9例は190週の時点でSD	13

2．治　療

びまん性脳幹部神経膠腫では，治療においてのみならず診断という意味においても手術の意義は認められていない[5]．

従って治療の中心はまず放射線照射ということになるが，通常の照射方法60 Gy/30 frによる生存期間は1年未満であることから，放射線照射の効果を増強する試みが精力的に行われてきた．

まず行われたのはhyperfractionation法である．放射線照射の1回線量を減らせば効果も減少するわけだが，この生物学的な効果は生物学的等価線量(biological effective dose, BED)という概念で評価される．下の式をみると分かるように，1回線量が減じるとBEDも減少するが，係数が違うために正常組織では腫瘍組織に比べてその減少の程度が大きい．そこで総線量を増加させるかわりに1回線量を少なくすることによって，正常組織の障害，特に晩期障害を極力抑えつつ抗腫瘍効果を高めようというアイデアである．

$$BED = nd\left(1+\frac{d}{\alpha/\beta}\right)$$

n：分割回数，d：1回線量，α と β は組織固有の値で，通常腫瘍では $\alpha/\beta=10$ Gy，正常組織では3 Gyという値を用いる[6]．

Hyperfractionation法は頭頸部癌等の領域で有効性が示されたが，びまん性脳幹部神経膠腫に対しても1980～90年代にかけて精力的に検証された(表2)[7~9]．しかし表2に示したように生存期間の延長は認められず，一方副作用として副腎皮質ステロイド投与の増加・遷延，血管障害，白質脳症，聴力障害，内分泌障害，痙攣などが報告され，結局その有効性は否定された形となっている[10]．

放射線照射の効果増強のもう一つの方法は化学療法との併用である(表3)．1980年代にrandomized studyが行われ放射線照射単独と放射線照射＋cisplatinの比較が行われた[11]．両者の間に生存期間の差は認められなかった．このデータでは生存期間中央値は両アームとも9ヵ月であるが5年生存率が放射線照射群17%，化学療法併用群23%とかなりよい成績になっている．これは当時はまだMRIが普及していなかったことから，表1に示したように脳幹部神

表 4　再発びまん性脳幹部神経膠腫に対する化学療法単独の成績

薬　剤	患者数	成　績	文献
Cyclophosphamide	5	4/5 PR	14
Oral VP-16	12	1/12 CR, 3/12 PR	15
5-FU, CCNU, HU, 6-MP	13	9/13 PR or SD 生存期間中央値 27 週	16
Temozolomide	21	7/21 SD 生存期間中央値 5.5ヵ月	17

経膠腫にも WHO grade が低く経過の長い症例群が含まれていることが認識されていなかったためにそのような症例も含まれていたことが理由と考えられる.

化学療法単独の成績としては，再発腫瘍を対象とした報告が多数存在する．その中で比較的成績のよいものを表4にまとめた．表をみていただくと分かるように，投与直後には腫瘍縮小効果がみられても直ぐに再増殖をきたすことが多く，生存期間からみると満足のゆく成績をあげた化学療法は存在しない．High-dose chemotherapy の報告も存在するが結果は惨憺たるものである[18].

通常の 60 Gy/30 fr の放射線照射を超える成績をあげている治療法がないことは，最新のレビューをみても明らかである[19]．特にびまん性脳幹部神経膠腫を対象とした臨床試験においては，通常組織診断がない故に，表1に示したような WHO grade の低い腫瘍である可能性のある病変を除外することが重要である．また画像所見と臨床所見の乖離がしばしばみられることから無増悪生存期間の定義には注意を要する[19]．これらは文献を読み解く場合にも重要である.

日々の臨床において，放射線照射による一時的な軽快の後まもなく悪化死亡への道をたどる患者を目の当たりにし，一日も早く，画期的な治療法が出現することを切望している.

文　献

1) Freeman CR, Perilongo G. Chemotherapy for brain stem glioma. Child's Nerv Syst. 1999；15：545-53.
2) 西川　亮. 小児神経膠腫. 脳腫瘍の診断と治療—最新の研究動向. 日本臨牀. 2005；63(増刊号 9)：183-7.
3) Robertson PI, Allen JC, Abbott IR, et al. Cervicomedullary tumors in children：a distinct subset of brainstem gliomas. Neurology. 1994；44：1798-803.
4) Yoshimura J, Onda K, Tanaka R, et al. Clinicopathological study of diffuse type brainstem gliomas：analysis of 40 autopsy cases. Neurol Med Chir(Tokyo). 2003；43：375-82.
5) Albright AL, Packer RJ, Zimmerman R, et al. Magnetic resonance scans should replace biopsies for the diagnosis of diffuse brain stem gliomas：a report from the Children's Cancer Group. Neurosurgery. 1993；33：1026-9.
6) 長谷川雄一，西尾正道，明神美弥子，他. 線量分割法の工夫—Algered Fractionation について. 癌と化学療法. 2006；33：428-35.
7) Freeman CR, Kapner J, Kun LE, et al. A detrimental effect of a combined chemotherapy-radiotherapy approach in children with diffuse intrinsic brain stem glioma? Int J Radiat Oncol Biol Phys. 2000；47：561-4.
8) Mandell LR, Kadota R, Freeman C, et al. There is no role for hyperfractionated radiotherapy in the management of children with newly diagnosed diffuse intrinsic brainstem tumors：results of a Pediatric Oncology Group phase III trial comparing conventional vs. hyperfractionated radiotherapy. Int J Radiat Oncol Biol Phys. 1999；43：959-64.
9) Packer RJ, Boyett JM, Zimmerman RA, et al. Outcome of children with brain stem gliomas after treatment with 7800 cGy of hyperfractionated radiotherapy. A Children's Cancer Group phase I/II trial. Cancer. 1994；74：1827-34.
10) Donaldson SS, Laningham F, Fisher PG. Advances toward an understanding of brainstem gliomas. J Clin Oncol. 2006；24：1266-72.
11) Jenkin RD, Boesel C, Ertel I, et al. Brain-stem tumors in childhood：a prospective randomized trial of irradiation with and without adjuvant CCNU, VCR and prednisone. A report from the Children's Cancer Study Group. J Neurosurg. 1987；66：227-33.
12) Wolff JEE, Molenkamp G, Lemmer A, et al. Oral chemotherapy for children with glioblastoma and brain stem tumors. Med Pediatr Oncol. 1997；29：413.
13) Walter AW, Gajjar A, Ochs JS, et al. Carboplatin and etoposide with hyperfractionated radiotherapy in children with newly diagnosed diffuse pontine gliomas：a phase I/II study. Med Ped Oncol. 1998；30：28-33.
14) Allen JC, Helson L. High-dose cyclophosphamide chemotherapy for recurrent CNS tumors in children. J Neurosurg. 1981；55：749-56.
15) Chamberlain MC. Recurrent brainstem gliomas treated with oral VP-16. J Neurooncol. 1993；15：133-9.
16) Rodriguez LA, Prados M, Fulton D, et al. Treatment of recurrent brain stem gliomas and other central nervous system tumors with 5-fluorouracil, CCNU, hydroxyurea and 6-mercaptopurine. Neurosurgery. 1988；22：692-3.
17) Lansford LS, Pearson ADJ, Thiesse P, et al. Efficacy of Temodal in diffuse intrinsic brain stem gliomas. Proc Am Soc Clin Oncol. 1998；17：A 2086.
18) Freeman CR, Perilongo G. Chemotherapy for brain stem gliomas. Child's Nerv Syst. 1999；15：545-53.
19) Hargrave D, Bartels U, Bouffet E. Diffuse brainstem glioma in children：critical review of clinical trials. Lancet Oncol. 2006；7：241-8.

Int. J. Radiation Oncology Biol. Phys., Vol. 68, No. 5, pp. 1388–1395, 2007

0360-3016/07/$–see front matter

ELSEVIER

doi:10.1016/j.ijrobp.2007.03.048

CLINICAL INVESTIGATION **Brain**

NEUROCOGNITIVE FUNCTION OF PATIENTS WITH BRAIN METASTASIS WHO RECEIVED EITHER WHOLE BRAIN RADIOTHERAPY PLUS STEREOTACTIC RADIOSURGERY OR RADIOSURGERY ALONE

HIDEFUMI AOYAMA, M.D., PH.D.,[a] MASAO TAGO, M.D., PH.D.,[b] NORIO KATO, M.D.,[a] TATSUYA TOYODA, M.D., PH.D.,[c] MASAHIRO KENJYO, M.D., PH.D.,[d] SAEKO HIROTA, M.D., PH.D.,[e] HIROKI SHIOURA, M.D., PH.D.,[f] TAISUKE INOMATA, M.D., PH.D.,[g] ETSUO KUNIEDA, M.D., PH.D.,[h] KAZUSHIGE HAYAKAWA, M.D., PH.D.,[i] KEIICHI NAKAGAWA, M.D., PH.D.,[b] GEN KOBASHI, M.D., PH.D.,[j] AND HIROKI SHIRATO, M.D., PH.D.[a]

[a]Department of Radiology, Hokkaido University Graduate School of Medicine, Sapporo; [b]Department of Radiology, University of Tokyo Hospital, Tokyo; [c]Department of Radiology, Kanto Medical Center Nippon Telegraph and Telephone East Corporation, Tokyo; [d]Department of Radiology, Hiroshima University School of Medicine, Hiroshima; [e]Department of Radiology, Hyogo Medical Center for Adults, Akashi; [f]Department of Radiology, Izumisano General Hospital, Izumisano; [g]Department of Radiology, Osaka Medical College, Osaka; [h]Department of Radiology, Keio University School of Medicine, Tokyo; [i]Department of Radiology, Kitasato University School of Medicine, Sagamihara; and [j]Department of Global Health and Epidemiology, Division of Preventive Medicine, Hokkaido University Graduate School of Medicine, Sapporo, Japan

Purpose: To determine how the omission of whole brain radiotherapy (WBRT) affects the neurocognitive function of patients with one to four brain metastases who have been treated with stereotactic radiosurgery (SRS).
Methods and Materials: In a prospective randomized trial between WBRT+SRS and SRS alone for patients with one to four brain metastases, we assessed the neurocognitive function using the Mini-Mental State Examination (MMSE). Of the 132 enrolled patients, MMSE scores were available for 110.
Results: In the baseline MMSE analyses, statistically significant differences were observed for total tumor volume, extent of tumor edema, age, and Karnofsky performance status. Of the 92 patients who underwent the follow-up MMSE, 39 had a baseline MMSE score of ≤27 (17 in the WBRT+SRS group and 22 in the SRS-alone group). Improvements of ≥3 points in the MMSEs of 9 WBRT+SRS patients and 11 SRS-alone patients ($p = 0.85$) were observed. Of the 82 patients with a baseline MMSE score of ≥27 or whose baseline MMSE score was ≤26 but had improved to ≥27 after the initial brain treatment, the 12-, 24-, and 36-month actuarial free rate of the 3-point drop in the MMSE was 76.1%, 68.5%, and 14.7% in the WBRT+SRS group and 59.3%, 51.9%, and 51.9% in the SRS-alone group, respectively. The average duration until deterioration was 16.5 months in the WBRT+SRS group and 7.6 months in the SRS-alone group ($p = 0.05$).
Conclusion: The results of the present study have revealed that, for most brain metastatic patients, control of the brain tumor is the most important factor for stabilizing neurocognitive function. However, the long-term adverse effects of WBRT on neurocognitive function might not be negligible.

Brain metastasis, Radiosurgery, Whole brain radiotherapy, Neurocognitive function, Leukoencephalopathy.

INTRODUCTION

Whole brain radiotherapy (WBRT) has long been a mainstay of treatment of brain metastases. The role of WBRT is to control radiologically visualized tumors, as well as nonvisualized micrometastases. Stereotactic radiosurgery (SRS) is a method of delivering high doses of focal irradiation to a tumor while minimizing the irradiation to the adjacent normal tissue (1, 2). Beginning in the 1990s, it has become increasingly used worldwide for patients with no more than a few brain metastases. A recent prospective randomized trial from the Radiation Therapy Oncology Group (RTOG) showed a small, but significant, improvement in the survival of patients who had had up to three metastases with good prognostic factors when SRS was used in conjunction with WBRT (2).

Reprint requests to: Hidefumi Aoyama, M.D., Ph.D., Department of Radiology, Hokkaido University Graduate School of Medicine, North 15, West 7, Kita-ku, Sapporo 060-8638, Japan. Tel: (+81) 11-716-1161; Fax: (+81) 11-706-7876; E-mail: hao@radi.med.hokudai.ac.jp

Partly supported by a grant-in-aid for scientific research (Grant 18209039) from the Japanese Ministry of Education, Culture, Sports, Science, and Technology.

Conflict of interest: none.

Received Feb 19, 2007, and in revised form March 26, 2007. Accepted for publication March 27, 2007.

However, WBRT has several adverse effects. Acute adverse effects include nausea and headache, but they are generally limited in severity and duration. However, the late adverse effects are severe, progressive, and irreversible. They are caused by a syndrome called leukoencephalopathy, which is a structural alteration of cerebral white matter in which myelin suffers the most damage. Mild cases are typified by a chronic confusional state with inattention, memory loss, and emotional dysfunction. More severe cases produce major neurologic sequelae such as dementia, abulia, stupor, and coma. These symptoms usually develop 6–24 months after cranial RT. The degree of neurotoxicity resulting from WBRT correlates with the total dose received and with the time-dose-fractionation scheme (3). Because of the concern about leukoencephalopathy resulting from WBRT, treatment strategies relying on SRS alone have been increasingly used (4–7). However, the omission of WBRT from the initial brain management has resulted in a significant increase in brain tumor recurrence (6, 7). Regine *et al.* (8) reported that brain tumor recurrence could also be a cause of neurocognitive functional deterioration.

The present study from the Japanese Radiation Oncology Study Group Protocol 99-1 is the first prospective randomized trial comparing SRS alone and WBRT combined with SRS. The details of the results have been previously published (1). In brief, it was a multi-institutional prospective randomized trial comparing WBRT+SRS and SRS alone conducted in Japan between 1999 and 2003. The 132 patients were randomized to receive WBRT+SRS (n = 65) or SRS alone (n = 67) for brain metastases. The primary endpoint was survival. No significant difference between the groups was observed in survival or cause of death; however, patients in the SRS-alone group developed brain tumor recurrences significantly more frequently than did those in the WBRT+SRS group. No difference in the functional observation rate (Karnofsky performance status ≥70) was observed.

We also monitored neurocognitive function serially using the Mini-Mental State Examination (MMSE) (8–12). We present the results of our detailed analysis of neurocognitive function for this trial. This is the first report to compare the neurocognitive function of patients who underwent either SRS alone or WBRT+SRS.

METHODS AND MATERIALS

Randomization and treatment

Eligible patients had one to four brain metastases detected on enhanced magnetic resonance imaging, each <3 cm, and a good systemic performance status (Karnofsky performance status of ≥70). A total of 132 patients were randomized to receive WBRT+SRS (65 patients) or SRS alone (67 patients) for brain metastases. Each patient provided written informed consent before entry into the study. Randomization was performed at the Hokkaido University Hospital Data Center. A permuted-blocks randomization algorithm was used with a block size of four. A randomization sheet was created for each institution. Before randomization, the patients were stratified according to the following criteria: number of brain metastases (single vs. two to four), extent of extracranial disease (active vs. stable), and primary tumor site (lung vs. other). Extracranial disease was considered to be stable when the tumor had been clinically controlled for ≥6 months before the detection of brain metastases. The WBRT schedule was 30 Gy in 10 fractions within 2–2.5 weeks. WBRT proceeded to SRS in patients assigned to the WBRT+SRS group. The SRS dose was prescribed to the tumor margin. Metastases with a maximal diameter of ≤2 cm were treated with 22–25 Gy, and those >2 cm were treated with 18–20 Gy. The dose was reduced by 30% when the treatment was combined with WBRT (1).

Assessment of neurocognitive function

Neurocognitive function was assessed using the MMSE (8–12). The MMSE is a short, standardized tool to grade cognitive function. The examination begins with an assessment of orientation to place and time. A maximum of 10 points can be obtained in this section. The memory test has the subject immediately repeat the name of three objects presented orally. The subject then subtracts 7s serially from 100 and is subsequently asked to recall the three items previously repeated. The final section evaluates aphasia and apraxia by testing naming, repetition, compliance with a three-step command, comprehension of written words, writing, and copying a drawing, for a total of 9 points in this section. The maximal score that can be obtained for the entire MMSE is 30 points (10–12). Physicians administered the MMSE before or during the brain treatment, again at 1 and 3 months after treatment and, if possible, every 3 months thereafter. The factors included in the analyses were the number of brain metastases on contrast-enhanced magnetic resonance imaging (MRI), the total volume of brain metastases, and the degree of brain edema on T_2-weighted MRI. Brain edema was scored from Grade 0 to 2. Patients with Grade 0 had no edema; those with Grade 1 had edema limited to less than one-half of one hemisphere, and those with Grade 2 had edema exceeding one-half of one hemisphere.

For the analysis of the post-treatment changes in the MMSE, patients for whom no follow-up MMSEs were available were excluded. A statistically meaningful change was defined as a three-point change in the MMSE score (8, 12). Although this criterion was thought to be potentially less conservative, owing to the possibility of missing a "meaningful" change in the MMSE score (13), it might be a more reliable change index (8, 12). In addition, a score of ≤26 was defined as abnormal (8). MRI findings regarding leukoencephalopathy were also assessed according to the criterion in the National Cancer Institute Common Toxicity Criteria, version 2.0, and correlated with the change in MMSE score (14). Tumor progression was scored when the tumor size had increased by at least 25% using the measurement of the perpendicular diameters (1).

Statistical analysis

The MMSE score was summarized as an average. Because of a ceiling effect and the clustering of values at 30, the data were not normally distributed. The Wilcoxon rank sum test was used to compare the mean values. The chi-square test was used to determine the relationship between two categorical variables, and Fisher's exact test was used when small cell sizes were encountered in 2 × 2 contingency tables. Univariate analyses were performed using the Kaplan-Meier method, and we used the log–rank test to compare differences between the groups. A two-sided p value of ≤0.05 was considered to reflect statistical significance. All statistical analyses were initially performed by a physician (H.A.) using a commercial statistical software package (StatView, version 5.0J, SAS Institute, Cary, NC), and all results were verified by a statistician

(G.K.) using a different software package (Statistical Analysis Systems, version 9.1, SAS Institute Japan, Tokyo, Japan).

RESULTS

Baseline MMSE

The pretreatment MMSE was available for 99 patients. MMSE data during the treatment were obtained for 11 additional patients. Those data, from 110 (83%) of the 132 patients enrolled in the study, constituted the "baseline" MMSE data and were used for the analysis (Fig. 1). The characteristics of those 110 patients are listed in Table 1 by treatment group. No statistically significant differences were found between the two groups. A comparison of the MMSE scores according to the patient characteristics is summarized in Table 2. The average baseline MMSE did not differ significantly between treatment groups (p = 0.47). Statistically significant differences were observed in the total tumor volume of brain metastases (<3 vs. ≥3 cm^3), extent of tumor edema (Grade 0-1 vs. Grade 2), age (<65 vs. ≥65 years), and Karnofsky performance status (70–80 vs. 90–100). The number of brain metastases was not a significant factor.

Post-treatment change in MMSE

Post-treatment improvement in MMSE. Follow-up MMSEs were given to 92 patients a median of 2.5 times (range, 1–17). The median follow-up period was 5.3 months (average, 11.0; range, 0.7–58.7). Of those 92 patients, 39 (17 in the WBRT+SRS group and 22 in the SRS-alone group) had a baseline MMSE score of ≤27. The 53 patients who had a baseline MMSE score of 28–30 were excluded from this analysis because an improvement of ≥3 points could not be expected (ceiling effect). The mean ± standard deviation MMSE value was 24.9 ± 3.3 in the WBRT+SRS group and 25.3 ± 2.1 in the SRS-alone group (p = 0.65). An improvement in MMSE of ≥3 points was observed in 20 (51%) of the 39 patients after the initial brain treatment. No statistically significant difference was found between the two treatment groups: 9 of 17 in the WBRT+SRS group and 11 of 22 in the SRS-alone group (chi-square = 0.03, p = 0.85). The improvement was observed at the mean of 6.0 ± 5.9 months in the WBRT+SRS group and 3.6 ± 2.8 months in the SRS-alone group (p = 0.24). Three patients experienced a worsening of MMSE (deterioration by ≥3 points) without improvement. The remaining 16 patients did not show a change of ≥3 points in their MMSE scores.

Post-treatment deterioration of MMSE. Included in this analysis were patients who had a baseline MMSE score of ≥27 (n = 65) and those whose baseline MMSE score was ≤26 but improved to ≥27 (n = 17) after the initial brain treatment. Because we found that some patients experience improvement in the MMSE after the initial brain treatment, we used the best MMSE score minus the deteriorated MMSE score for the change in MMSE for this analysis. The Kaplan-Meier curves of the patients who did not have a 3-point deterioration in the MMSE score in each treatment group are shown in Fig. 2a. No statistically significant difference was found by log–rank test (p = 0.73). Deterioration of the MMSE score occurred in 14 of 36 patients in the WBRT+SRS group and 12 of 46 in the SRS-alone group (chi-square =1.52, p = 0.21). However, the time until the deterioration was marginally different between the two groups. Deterioration was observed at an average of 13.6 months (median, 12.0; range, 1.8–31.1) in the WBRT+SRS group and 6.8 months (median, 6.6; range, 1.6–12.9) in the SRS-alone group (p = 0.05). The deterioration was presumably attributed to brain tumor recurrence in 3 and 11 patients in the WBRT+SRS and SRS-alone groups, respectively (p < 0.0001). The deterioration was either clinically or radiologically attributed to a toxic radiation event in 5 and 0 patients in the WBRT+SRS and SRS-alone groups, respectively. The cause was unclear in the remaining 7 patients. An additional follow-up MMSE after the 3-point decrease was available for 10 of 26 patients. Of those 10, an improvement of ≥3 points was observed in 7 (5 in the WBRT+SRS group and 2 in the SRS-alone group). Of the 7 patient, 2 underwent salvage brain treatment (1 with SRS and 1 with surgery). The other 5 patients received only close observation or best supportive care, including steroid administration. Figure 2b shows the

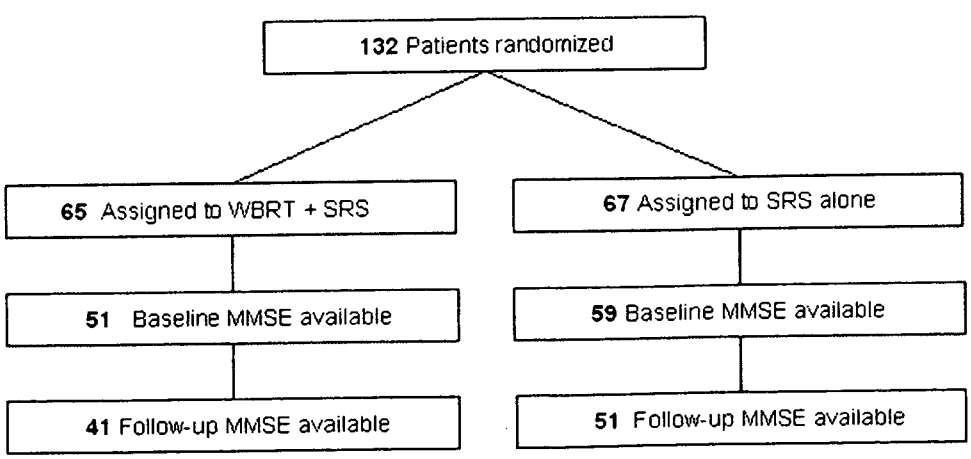

Fig. 1. Flow chart of study participants. WBRT = whole brain radiotherapy; SRS = stereotactic radiosurgery; MMSE = Mini-Mental State Examination.

Table 1. Baseline patient characteristics

Characteristic	WBRT+SRS (n = 51)	SRS (n = 59)	p
Age at diagnosis (y)			0.71
Median	65	64	
Range	36–78	33–81	
<65 y	25 (49)	31 (52)	
≥65 y	26 (51)	28 (48)	
Gender			0.37
Men	36 (71)	46 (78)	
Women	15 (29)	13 (22)	
Karnofsky performance status			0.22
70–80	24 (47)	21 (36)	
90–100	27 (53)	38 (64)	
No. of brain metastases			0.82
1	27 (53)	30 (51)	
2–4	24 (47)	29 (49)	
Brain edema			0.63
Grade 0	13 (25)	14 (24)	
Grade 1	29 (57)	38 (64)	
Grade 2	9 (18)	7 (12)	
Total volume of brain metastases (cm^3)			0.67
<3	23 (45)	29 (49)	
≥3	28 (55)	30 (51)	
Primary tumor site			0.71
Lung	32 (63)	39 (66)	
Other	19 (37)	20 (34)	
Primary tumor status			0.54
Stable	23 (45)	30 (51)	
Active	28 (55)	29 (49)	
Extracranial metastases			0.40
Stable	35 (69)	36 (61)	
Active	16 (31)	23 (39)	

Abbreviations: WBRT = whole brain radiotherapy; SRS = stereotactic radiosurgery.

Data presented as number of patients, with percentages in parentheses, unless otherwise noted.

Table 2. Analysis of baseline MMSE score and associated factors

Variable	n	Average (SD)	p (Mann-Whitney U test)
Treatment group			0.86
WBRT+SRS	51	26.7 (3.3)	
SRS alone	59	27.1 (2.9)	
Age at diagnosis (y)			0.001
<65	56	27.9 (2.0)	
≥65	54	25.9 (3.7)	
Gender			0.33
Men	82	26.7 (3.3)	
Women	28	27.6 (2.1)	
Karnofsky performance status			0.0002
70–80	45	25.5 (3.8)	
90–100	65	27.9 (1.9)	
No. of brain metastases			0.29
1	57	27.4 (2.3)	
2–4	53	26.4 (3.7)	
Brain edema			
Grade 0-1	94	27.2 (2.8)	
Grade 2	16	25.0 (4.2)	
Total volume of brain metastases (cm^3)			0.01
<3	52	27.8 (1.9)	
≥3	58	26.1 (3.7)	
Primary tumor site			0.86
Lung	71	26.9 (3.2)	
Other	39	27.0 (2.9)	
Extracranial disease			0.96
Stable	23	27.6 (2.2)	
Active	87	27.2 (2.2)	

Abbreviations: MMSE = Mini-Mental State Examination; SD = standard deviation; other abbreviations as in Table 1.

Kaplan-Meier curves of patients free of MMSE deterioration when the first event in a decrease was not counted if the MMSE showed significant recovery with additional follow-up. The 12-, 24-, and 36-month actuarial free rate of a second event in the 3-point decrease in the MMSE score was 76.1% (95% confidence interval [CI], 58.7–93.5), 68.5% (95% CI, 47.3–89.7), and 14.7% (95% CI, 0–39.0) in the WBRT+SRS group and 59.3% (95% CI, 37.5–81.1), 51.9% (95% CI, 28.6–75.2), and 51.9% (95% CI, 28.6–75.2) in the SRS-alone group, respectively. Although the difference was not significant by the log–rank test (p = 0.79), the separation of the two curves at between 12 and 24 months became wider than that in Fig. 2a. The average duration until deterioration was 16.5 months (median, 15.8; range, 1.8–34.5) in the WBRT+SRS group and 7.6 months (median, 7.4; range, 1.6–12.9) in the SRS-alone group (p = 0.05).

Figure 2c shows the actuarial rate of subjects free from a decrease in the MMSE score to ≤26. An event of a decrease to ≤26 was counted as an event unless the MMSE score recovered to ≥27 with additional follow-up. The 12-, 24-, and 36-month actuarial MMSE preservation rate (≥27) was 78.8% (95% CI, 61.6–96.0), 78.8% (95% CI, 61.6–96.0), and 22.5% (95% CI, 0–49.4) in the WBRT+SRS group and 53.3% (95% CI, 32.9–73.7), 42.6% (95% CI, 17.9–67.3), and 42.6% (95% CI, 17.9–67.3) in the SRS-alone group, respectively (p = 0.46). The separation of the two curves at between 12 and 24 months after treatment became more prominent than that in Fig. 2b. This fact might indicate that WBRT was effective at preventing the deterioration of neurocognitive function resulting from brain tumor recurrence in an early phase after treatment. However, WBRT could be a cause of continuous deterioration of neurocognitive function in long-term survivors.

The relationship between the MRI findings of leukoencephalopathy using the National Cancer Institute Common Toxicity Criteria, version 2, and clinical manifestations was also evaluated. Abnormal MRI-determined leukoencephalopathy was seen in 7 patients (Grade 1 in 2 patients, Grade 2 in 4, and Grade 3 in 1). All 7 patients were in the WBRT+SRS group. Four of them (Grade 1 in 1 patient, Grade 2 in 2, and Grade 3 in 1) experienced a clinically significant decrease in the MMSE score (≥3 points). The other 3 patients (Grade 1 in 1 and Grade 2 in 2) did not experience a significant decrease in the MMSE score. Fig. 3 shows illustrative MRI scans of 2 patients with different clinical courses.

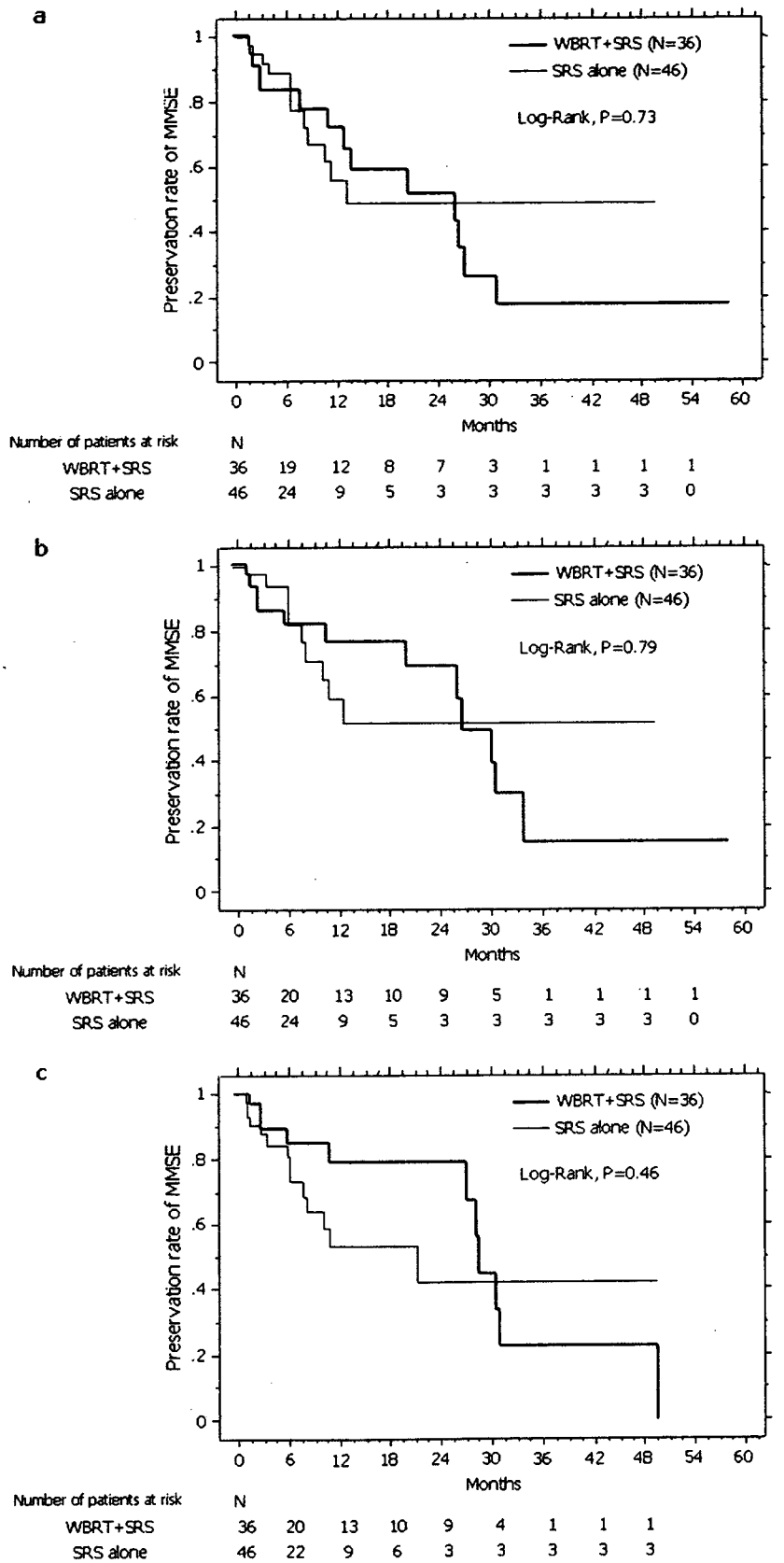

Fig. 2. (a) Actuarial curves of subjects free from 3-point decrease in Mini-Mental State Examination (MMSE). (b) Actuarial curves of subjects free from second 3-point decrease in MMSE. (c) Actuarial rate of subjects free from decrease of MMSE to ≤26. WBRT = whole brain radiotherapy; SRS = stereotactic radiosurgery.

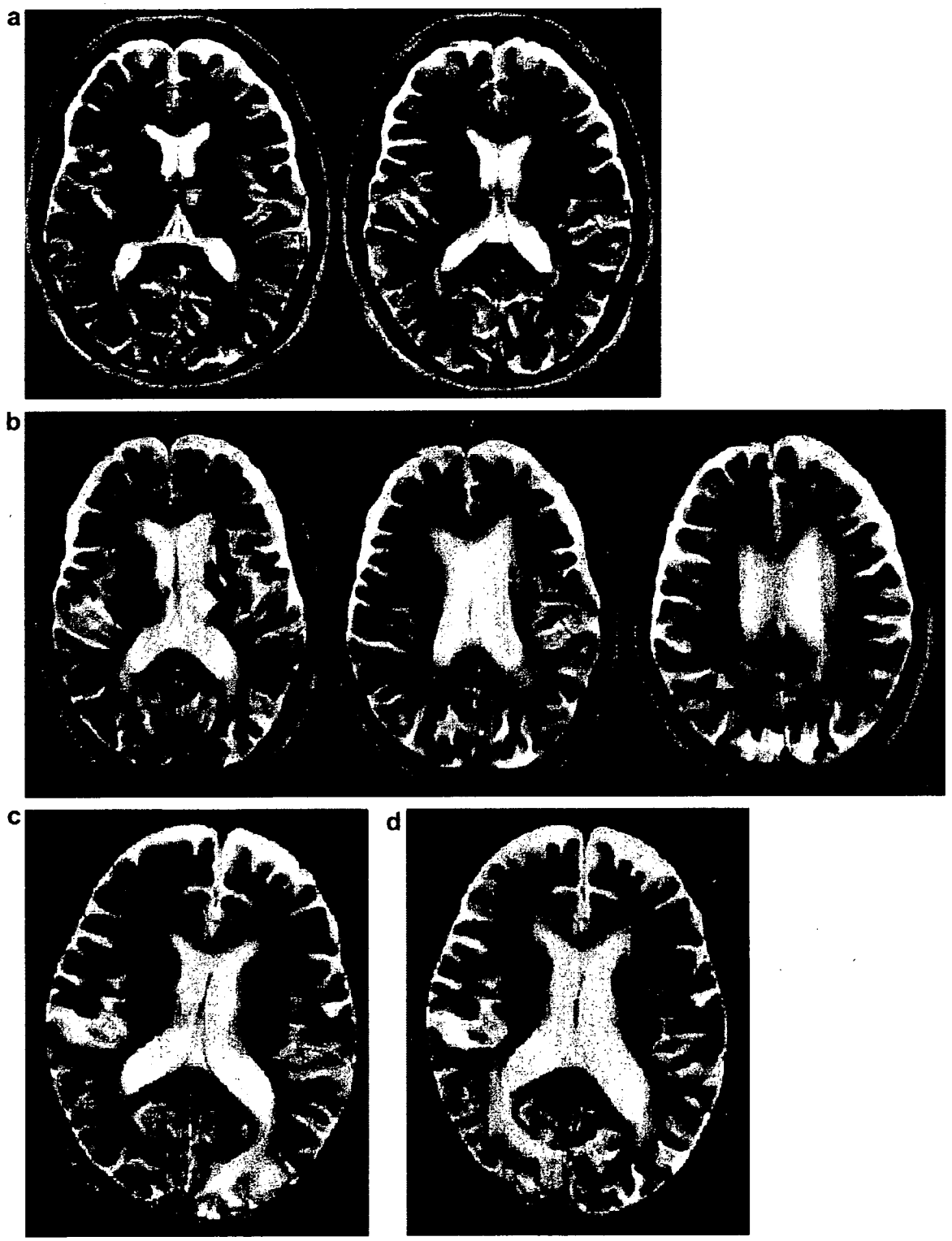

Fig. 3. (a) Pretreatment T_2-weighted magnetic resonance imaging (MRI) study of Patient 1, who then underwent whole brain radiotherapy (WBRT) plus stereotactic radiosurgery (SRS). (b) T_2-weighted MRI scan of Patient 1 at 46.6 months after initial brain treatment. (c) Pretreatment T_2-weighted MRI study of Patient 2, who then underwent WBRT plus SRS. (d) T_2-weighted MRI scan of Patient 2 at 15 months after initial brain treatment.

Patient 1 experienced Grade 3 radiologic leukoencephalopathy without tumor recurrence at 47 months after WBRT+SRS (Fig. 3a, b). This patient had a baseline MMSE score of 29 and a best score of 30 at 7 months after RT. She experienced a continuous decrease in the MMSE score after a transient recovery, and her last MMSE score, at 47 months, was 21. Patient 2 experienced Grade 2 radiologic leukoencephalopathy at 15 months after WBRT+SRS. His baseline MMSE score was 29 and his final score, at 15 months, was 29 (Fig. 3c, d).

DISCUSSION

The MMSE is the most frequently used and established tool for assessing the neurocognitive function of patients with brain tumors (7–13). The importance of MMSE in the treatment of patients with brain metastases, as well as in those with low-grade glioma, has been reported by Murray *et al.* (9) and Brown *et al.* (10). Murray *et al.* (9) assessed the MMSE scores of 182 patients with brain metastases who were treated with WBRT to 30 Gy in 10 fractions among 445 patients enrolled in a RTOG study (RTOG 91-04), in which 30 Gy in 10 fractions was compared with accelerated hyperfractionation of 54.4 Gy (1.6 Gy twice daily). They reported that patients who had low MMSE score (≤23) had a worse prognosis than those with greater MMSE scores. In 88 patients who had a baseline MMSE score of ≤29, 48 (54.5%) demonstrated an improvement in the MMSE score at a follow-up visit. Regine *et al.* (8) evaluated 309 patients whose MMSE scores were available among 445 patients who were enrolled in RTOG 91-04. They found that control of the brain tumor had a significant impact on the maintenance of the MMSE scores. At 3 months, the average change in MMSE score was a decline of 0.5 for those whose brain metastases were radiologically controlled compared with a decline of 6.3 for those with uncontrolled brain metastases ($p = 0.02$). One of the shortcomings of their report was that they evaluated the change in MMSE only at 3 months after brain treatment; therefore, the long-term effect of WBRT was not fully investigated. In the present study, we found some important factors that might affect a patient's baseline MMSE score. The number of brain metastases was not a significant factor affecting the baseline MMSE score, but tumor volume (≥3 cm^3) and degree of edema (one-half of one hemisphere or more) were significant factors. More importantly, 51% of patients who had an MMSE score of ≤27 experienced significant improvement in the MMSE score at a median of 2.7 months after treatment, regardless of which treatment they had initially received. This finding supports the findings reported by Murray *et al.* (9).

Another important finding of the present study was the continuous decrease in MMSE score in patients who underwent WBRT initially, although WBRT was not a cause of neurocognitive deterioration for most brain metastatic patients. Patients who received WBRT combined with SRS experienced a stable MMSE score for approximately 2 years after treatment, perhaps because of the preventative effect on brain tumor recurrence compared with SRS alone. Considering that the median survival of patients with brain metastases is about 7 months, this prevention effect when WBRT is included in the initial management is beneficial for most brain metastatic patients. Nevertheless, the continuous deterioration of neurocognitive function for long-term survivors who underwent WBRT should not be neglected.

In addition, the MRI findings suggestive of leukoencephalopathy were useful only for patients who experienced severe neurocognitive dysfunction. Most patients who had Grade 1-2 radiologic leukoencephalopathy did not show clinically meaningful signs of neurocognitive dysfunction as assessed by the MMSE. This is consistent with the findings of Fujii *et al.* (15). They evaluated the white matter changes on MRI after WBRT in 24 patients. Although 12 patients (50%) developed radiologic Grade 3 (large confluent areas) or worse leukoencephalopathy, only 6 of these 12 patients had clinical abnormalities such as dementia, depression, and speech impairment. However, the true incidence of neurocognitive deterioration is not well understood. In patients with small cell carcinoma of the lung whose primary tumor is in complete remission, prophylactic cranial irradiation (PCI) using WBRT is becoming a standard treatment (16). van de Pol *et al.* (17) assessed late neurologic toxicity in 7 patients who received PCI and survived ≥2 years. The memory decline was insidious and started within 6 months after the termination of therapy in 4 patients and after 2 years in 2 patients (17). Stuschke *et al.* (18) reported that patients treated with PCI had higher grade white matter abnormalities than patients who were not treated with PCI, as detected by T_2-weighted MRI ($p = 0.04$). Grade 4 white matter abnormalities were detected in 2 of 9 patients treated with PCI and in 0 of 4 patients not treated with PCI (18). Cull *et al.* (19) reported the frequency of neurocognitive impairment in 52 patients who received PCI and survived >2 years. They evaluated neurocognitive function using four different methods: the Williams delayed recall test, the Digit symbol, the Complex figure test, and Trials A and B. No impairment in any of these tests was observed in 19% of patients. Impairment was observed with one test in 27%, two tests in 22%, three tests in 25%, and all four tests in 7% (19). These findings indicate that WBRT frequently accompanies neurocognitive impairment in long-term survivors.

Although our findings are of interest, our report was not without limitations. First, we did not monitor the use of corticosteroids, which could potentially influence neurocognitive function. Second, we used MMSE as the sole measurement of neurocognitive function; however, the MMSE has been criticized for having low specificity and sensitivity (20). Recently, the RTOG began using a "neurocognitive battery" of several assessment tools (21–24). Mehta *et al.* (21, 22) suggested that this battery is feasible for use in clinical trials and could detect small changes in neurocognitive function that the MMSE alone could not detect. Nevertheless, we believe the present findings are valuable and that the MMSE is still a useful tool to examine neurocognitive function in trials in which neurocognitive function is not the primary endpoint. No established effective treatment is available for neurocognitive deterioration after WBRT. Recently, Shaw *et al.* (25) reported that donepezil, a drug developed for Alzheimer's disease, has a positive effect on cognitive function; however, additional investigation is necessary to establish this drug's potential role in relation to WBRT.

CONCLUSION

The results of the present study have revealed that the control of brain tumors is the most important factor in stabilizing

neurocognitive function for most brain metastatic patients. However, the long-term adverse effect on neurocognitive function might not be negligible. Therefore, the development of a method to identify those patients who are less likely to experience brain tumor recurrence, as well as additional investigation to establish an optimal schedule of WBRT when combined with SRS, are important steps toward the refinement of the treatment of brain metastases.

REFERENCES

1. Aoyama H, Shirato H, Tago M, *et al.* Stereotactic radiosurgery plus whole-brain radiation therapy vs. stereotactic radiosurgery alone for treatment of brain metastases: A randomized controlled trial. *JAMA* 2006;295:2483–2491.
2. Andrews DW, Scott CB, Sperduto PW, *et al.* Whole brain radiation therapy with or without stereotactic radiosurgery boost for patients with one to three brain metastases: Phase III results of the RTOG 9508 randomised trial. *Lancet* 2004;363:1665–1672.
3. Filley CM, Kleinschmidt-DeMasters BK. Toxic leukoencephalopathy. *N Engl J Med* 2001;345:425–432.
4. Hasegawa T, Kondziolka D, Flickinger JC, *et al.* Brain metastases treated with radiosurgery alone: An alternative to whole brain radiotherapy? *Neurosurgery* 2003;52:1318–1326.
5. Yamamoto M, Ide M, Nishio S, *et al.* Gamma knife radiosurgery for numerous brain metastases: Is this a safe treatment? *Int J Radiat Oncol Biol Phys* 2002;53:1279–1283.
6. Sneed PK, Suh JH, Goetsch SJ, *et al.* A multi-institutional review of radiosurgery alone vs. radiosurgery with whole brain radiotherapy as the initial management of brain metastases. *Int J Radiat Oncol Biol Phys* 2002;53:519–526.
7. Aoyama H, Shirato H, Onimaru R, *et al.* Hypofractionated stereotactic radiotherapy alone without whole brain irradiation for patients with solitary and oligo brain metastasis using non-invasive fixation of the skull. *Int J Radiat Oncol Biol Phys* 2003;56:793–800.
8. Regine WF, Scott C, Murray K, *et al.* Neurocognitive outcome in brain metastases patients treated with accelerated-fractionation vs. accelerated-hyperfractionated radiotherapy: An analysis from Radiation Therapy Oncology Group Study 91-04. *Int J Radiat Oncol Biol Phys* 2001;51:711–717.
9. Murray KJ, Scott C, Zachariah B, *et al.* Importance of the mini-mental status examination in the treatment of patients with brain metastases: A report from the Radiation Therapy Oncology Group protocol 91-04. *Int J Radiat Oncol Biol Phys* 2000;48: 59–64.
10. Brown PD, Buckner JC, O'Fallon JR, *et al.* Effects of radiotherapy on cognitive function in patients with low-grade glioma measured by the Folstein Mini-Mental State Examination. *J Clin Oncol* 2003;21:2519–2524.
11. Folstein MF, Folstein SE, McHugh PR. "Mini-mental state": A practical method for grading the cognitive state of patients for the clinician. *J Psychiatr Res* 1975;12:189–198.
12. Crum RM, Anthony JC, Bassett SS, *et al.* Population-based norms for the Mini-Mental State Examination by age and educational level. *JAMA* 1993;269:2386–2391.
13. Temkin NR, Heaton RK, Grant I, *et al.* Detecting significant change in neuropsychological test performance: A comparison of four models. *J Int Neuropsychol Soc* 1999;5:357–369.
14. RTOG/EORTC late radiation morbidity scoring schema. Available at: http://www.rtog.org/members/toxicity/late.html. Accessed June 15, 1999.
15. Fujii O, Tsujino K, Soejima T, *et al.* White matter changes on magnetic resonance imaging following whole-brain radiotherapy for brain metastases. *Radiat Med* 2006;24:345–350.
16. Auperin A, Arriagada R, Pignon JP, *et al.*, for the Prophylactic Cranial Irradiation Overview Collaborative Group. Prophylactic cranial irradiation for patients with small-cell lung cancer in complete remission. *N Engl J Med* 1999;341:476–484.
17. van de Pol M, ten Velde GP, Wilmink JT, *et al.* Efficacy and safety of prophylactic cranial irradiation in patients with small cell lung cancer. *J Neurooncol* 1997;35:153–160.
18. Stuschke M, Eberhardt W, Pottgen C, *et al.* Prophylactic cranial irradiation in locally advanced non-small-cell lung cancer after multimodality treatment: Long-term follow-up and investigations of late neuropsychologic effects. *J Clin Oncol* 1999;17: 2700–2709.
19. Cull A, Gregor A, Hopwood P, *et al.* Neurological and cognitive impairment in long-term survivors of small cell lung cancer. *Eur J Cancer* 1994;30:1067–1074.
20. Meyers CA, Wefel JS. The use of the Mini-Mental State Examination to assess cognitive functioning in cancer trials: No ifs, ands, or buts, or sensitivity. *J Clin Oncol* 2003;21:3557–3558.
21. Mehta MP, Shapiro WR, Glantz MJ, *et al.* Lead-in phase to randomized trial of motexafin gadolinium and whole brain radiation for patients with brain metastases: Centralized assessment of magnetic resonance imaging, neurocognitive, and neurologic end points. *J Clin Oncol* 2002;20:3445–3453.
22. Mehta MP, Rodrigus P, Terhaard CH, *et al.* Survival and neurologic outcomes in a randomized trial of motexafin gadolinium and whole-brain radiation therapy in brain metastases. *J Clin Oncol* 2003;21:2529–2536.
23. Meyers CA, Smith JA, Bezjak A, *et al.* Neurocognitive function and progression in patients with brain metastases treated with whole brain radiation and motexafin gadolinium: Results of a randomized phase III trial. *J Clin Oncol* 2004;22:157–165.
24. Regine WF, Schmitt FA, Scott CB, *et al.* Feasibility of neurocognitive outcome evaluations in patients with brain metastases in a multi-institutional cooperative group setting: Results of Radiation Therapy Oncology Group trial BR-0018. *Int J Radiat Oncol Biol Phys* 2004;58:1346–1352.
25. Shaw EG, Rosdhal R, D'Agostino RB Jr., *et al.* Phase II study of donepezil in irradiated brain tumor patients: Effect on cognitive function, mood, and quality of life. *J Clin Oncol* 2006;24: 1415–1420.

Radiat Med (2007) 25:430–431
DOI 10.1007/s11604-007-0168-9

LETTER TO THE EDITOR

Matrixmetalloproteinases: up-regulated in subclones that survived 10-Gy irradiation

Takeshi Nishioka · Motoaki Yasuda · Kaori Tsutsumi
Hisashi Haga · Hiroki Shirato

Received: May 14, 2007 / Accepted: June 29, 2007

We report an interesting finding regarding the mRNA expression pattern of cell lines that survived 10-Gy irradiation. According to the linear quadratic model in a textbook, the survival curve shows a straight line at high-dose areas, meaning that cells are killed at a constant rate. The model explains that there are two types of killing: α-killing, which is a function of dose D, and β-killing, which is a function of D^2. This is a kind of modified version of a hit model wherein some percentage of cells remain intact after irradiation.

We used mouse fibrosarcoma cells (QRsP, p53 wild type); 1×10^4 cells were exposed to 10 Gy. At day 12, we harvested 6 of about 30 colonies and established them as QRsPIR-1 to QUsPIR-6. cDNA microarray analysis was performed for the parental QRsP and QRsPIR-1. The pattern was significantly different between the two, suggesting that the cells that survived were not intact. Rather, they had a more aggressive nature than the parental QRsP: matrix metalloproteinase (MMP)13 (collagenase) and MMP3 were significantly up-regulated (26-fold and 23-fold, respectively). These results encouraged us to perform an in vivo study in which 2×10^4 cells were injected subcutaneously into the flanks of C57BL/6 mice (five animals each). At day 28, a large tumor mass was palpated in each of the five mice for QRSPIR-1. In contrast, only two mice developed a tumor mass of the parental QRsP. To form a tumor mass, degradation of surrounding tissue (mainly collagen) must be done. Our findings are quite revealing in this regard.

To see whether up-regulation of MMP is a rare event, we performed cDNA analysis for QRsPIR-5 and an in vitro 10-Gy irradiation experiment for human lung adenocarcinoma H1299 (p53 mutant) and human lung carcinoma A549 (p53 wild type) in a similar manner. Interestingly, MMP13 and MMP3 were up-regulated 4.0- and 6.4-fold, respectively, for QRsPIR-5. Although the changes were not as significant as for QRsPIR-1, the values were still large compared to other published DNA array data. We randomly selected IR-1 and IR-5 for array analysis. (other IR clones were left untouched because of the high cost of each array analysis, and it is possible that these other IR clones would have a similar pattern if we had performed the analysis on them.) MMP1 (collagenase) was up-regulated 4.4-fold and 2.0-fold for H1299-IR and A549-IR, respectively. In A549-IR, MMP7 (matrilysin) was also up-regulated 2.8-fold.

It should be emphasized that none of the MMP family was included in the down-regulated gene lists of our four array analyses. Recently, it has been reported that MMPs not only play an important role in tumor invasion but also enhance cell motility,[1–3] both of which are important characteristics of malignant tumor cells. In fact, a cell

T. Nishioka (✉) · K. Tsutsumi
Laboratory of Radiation Therapy, School of Medicine, Hokkaido University, N12W5, Kita-ku, Sapporo 060-0812, Japan
Tel./Fax +81-11-706-3411
e-mail: trout@radi.med.hokudai.ac.jp

M. Yasuda
Department of Oral Pathobiological Science, Graduate School of Dental Medicine, Hokkaido University, Sapporo, Japan

H. Haga
Division of Biological Sciences, Graduate School of Science, Hokkaido University, Sapporo, Japan

H. Shirato
Department of Radiology, Graduate School of Medicine, Hokkaido University, Sapporo, Japan

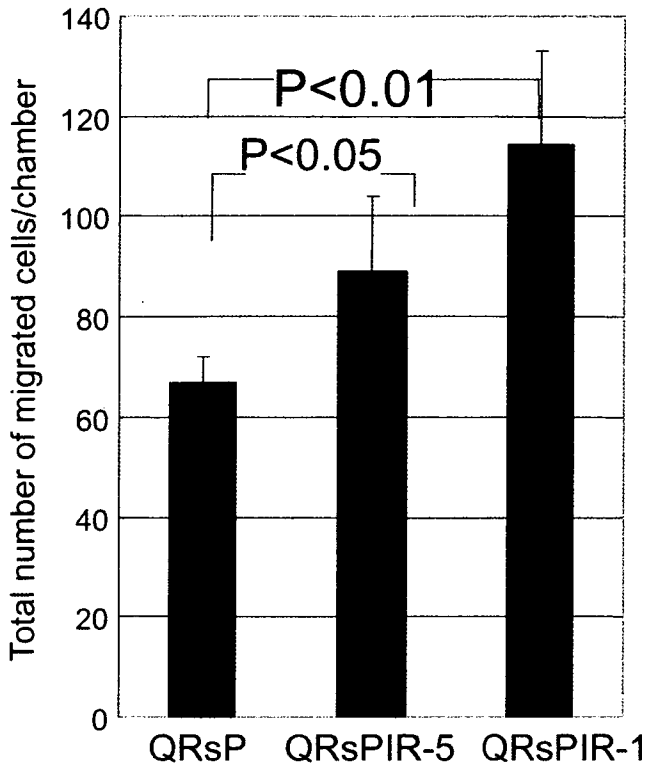

Fig. 1. Boyden chamber cell motility assay

motility assay using the Boyden chamber demonstrated increased cell motility for IR clones (Fig. 1). Cell motility was higher for QRsPIR-1 than for QRsPIR-5, which implies that MMPs are associated with cell movement.

In conclusion, all of our four cDNA array analyses showed up-regulation of MMPs. Irradiation is an effective means of cancer therapy, but it should be taken into consideration that surviving cells acquire a more aggressive nature.

References

1. López-Rivera E, Lizarbe TR, Martínez-Moreno M, López-Novoa JM, Rodríguez-Barbero A, et al. Matrix metalloproteinase 13 mediates nitric oxide activation of endothelial cell migration. Proc Natl Acad Sci U S A 2005;102:3685–90.
2. Sossey-Alaoui K, Ranalli TA, Li X, Bakin AV, Cowell JK. WAVE3 promotes cell motility and invasion through the regulation of MMP-1, MMP-3, and MMP-9 expression. Exp Cell Res 2005;308:135–45.
3. Remy L, Trespeuch C, Bachy S, Scoazec JY, Rousselle P. Matrilysin 1 influences colon carcinoma cell migration by cleavage of the laminin-5 beta3 chain. Cancer Res 2006;66: 11228–37.

Int. J. Radiation Oncology Biol. Phys., Vol. 69, No. 2, pp. 376–380, 2007

0360-3016/07/$–see front matter

ELSEVIER

doi:10.1016/j.ijrobp.2007.03.042

CLINICAL INVESTIGATION **Liver**

INTERCEPTING RADIOTHERAPY USING A REAL-TIME TUMOR-TRACKING RADIOTHERAPY SYSTEM FOR HIGHLY SELECTED PATIENTS WITH HEPATOCELLULAR CARCINOMA UNRESECTABLE WITH OTHER MODALITIES

HIROSHI TAGUCHI, M.D.,* YUSUKE SAKUHARA, M.D.,* SHUHEI HIGE, M.D.,† KEI KITAMURA, M.D.,* YASUHIRO OSAKA, M.D.,* DAISUKE ABO, M.D.,* DAICHI UCHIDA, M.D.,* AKIHIRO SAWADA, M.D.,* TOSHIYA KAMIYAMA, M.D.,‡ TADASHI SHIMIZU, M.D.,* HIROKI SHIRATO, M.D.,* AND KAZUO MIYASAKA, M.D.*

Departments of *Radiology, †Gastroenterology, and ‡General Surgery, Hokkaido University School of Medicine, Sapporo, Japan

Purpose: To assess the clinical outcome of intercepting radiotherapy, in which radiotherapy is delivered only when a tumor in motion enters a target area, using a real-time tumor-tracking radiotherapy (RTRT) system for patients with hepatocellular carcinoma who were untreatable with other modalities because the tumors were adjacent to crucial organs or located too deep beneath the skin surface.

Methods and Materials: Eighteen tumors, with a mean diameter of 36 mm, were studied in 15 patients. All tumors were treated on a hypofractionated schedule with a tight margin for setup and organ motion using a 2.0-mm fiducial marker in the liver and the RTRT system. The most commonly used dose of radiotherapy was 48 Gy in 8 fractions. Sixteen lesions were treated with a BED_{10} of 60 Gy or more (median, 76.8 Gy).

Results: With a mean follow-up period of 20 months (range, 3–57 months), the overall survival rate was 39% at 2 years after RTRT. The 2-year local control rate was 83% for initial RTRT but was 92% after allowance for reirradiation using RTRT, with a Grade 3 transient gastric ulcer in 1 patient and Grade 3 transient increases of aspartate amino transaminase in 2 patients.

Conclusions: Intercepting radiotherapy using RTRT provided effective focal high doses to liver tumors. Because the fiducial markers for RTRT need not be implanted into the tumor itself, RTRT can be applied to hepatocellular carcinoma in patients who are not candidates for other surgical or nonsurgical treatments. © 2007 Elsevier Inc.

Radiotherapy, Liver, Hepatocellular carcinoma, Real-time tumor-tracking radiotherapy.

INTRODUCTION

There are a number of nonsurgical local treatment techniques for the ablation of hepatocellular carcinoma (HCC), including radiofrequency ablation (RFA), percutaneous ethanol injection (PEI), and cryosurgery (1). These techniques require direct insertion of a needle or probe into the tumor mass. However, with HCC at deep locations, such as the top of the dome, near the inferior vena cava, or near the main portal vein, a needle or probe often cannot be inserted at the proper position. Transarterial embolization (TAE) is applicable only when one can identify the feeding artery, which is often difficult (2).

Radiotherapy has been a palliative treatment for patients with unresectable advanced HCC, but conventional radiotherapy is limited by the liver's low tolerance to large volumes of irradiation (3). Both focal radiotherapy using narrow-beam X-ray and particle therapy are expected to be useful for reducing radiation-induced liver damage (RILD) (4). When the tumor is close to the gastrointestinal (GI) tract, radiation-induced GI ulcer is a dreadful complication (5). Moreover, it is hard to increase the dose to the HCC when the tumor is in that position, owing to the large respiratory movement of the liver. In particle therapy, such as proton and carbon ion treatment, respiratory gating systems have been used to reduce the volume of normal tissue in the irradiated volume. As a result, the dose to the GI tract might be reduced in the particle therapy (6, 7).

In 1999 we began using a real-time tumor-tracking radiotherapy (RTRT) system to increase the accuracy of the nonsurgical treatment of tumors in motion (8). This has made intercepting radiotherapy possible for tumors in motion, whereby the tumor is irradiated only when it enters a target area, with a certain amount of permitted dislocation. After developing a technique to percutaneously insert a 2.0-mm gold

Reprint requests to: Hiroshi Taguchi, M.D., Department of Radiology, Hokkaido University Hospital, North-15 West-7, Sapporo 060-8638, Japan. Tel: (+81) 11-706-5975; Fax: (+81) 11-706-7876; E-mail: thiroshi@radi.med.hokudai.ac.jp

Supported by Grants-in-Aid from the Ministry of Education, Culture, Sports, and Technology in Japan (No. 18209039, No. 17016002).

Conflict of interest: none.

Received Oct 30, 2006, and in revised form Feb 27, 2007. Accepted for publication March 2, 2007.

fiducial marker into the liver and to confirm its localization stability (9), we suggested that intercepting radiotherapy using RTRT can be a radical radiotherapy for primary HCC (10). Because the fiducial marker does not need to be inserted directly into the tumor when RTRT is used, this method is applicable to more patients than is the case with percutaneous focal ablation techniques, such as RFA and cryosurgery. However, we have restricted the indication of RTRT to patients who were not eligible for other nonsurgical treatment techniques. In the present study, the outcomes of patients treated with the RTRT technique in the last 5 years were retrospectively analyzed to determine its proper indications for HCC.

METHODS AND MATERIALS

The focus of this study was on primary HCC diagnosed by dynamic computed tomography (CT) with the aid of serum tumor marker, according to the noninvasive Barcelona criteria (11). Patients were candidates if they were not eligible for any other treatment, such as surgery, RFA, PEI, and TAE. They were required to be 80 years old or younger and to have a Karnofsky performance status of 70% or more, as well as a liver function equivalent to Class A or B in the Child classification. Patients were excluded if they had uncontrolled ascites, obstructive jaundice, active gastroenteric bleeding, or a tendency to bleed. Patients who had tumor thrombosis of the portal vein or extrahepatic active metastatic disease on imaging examination were also excluded.

Multidetector CT was taken with a breath hold at the end of the expiratory phase of normal breathing. The slice thickness and interval were 2 mm. Gross tumor volume (GTV) was chosen to be compatible with the enhanced area in the early arterial phase of dynamic CT. Clinical target volume (CTV) was GTV plus a 5-mm margin three-dimensionally; thus the CTV diameter was 10 mm larger than the GTV. Planning target volume (PTV) was CTV plus a 5-mm margin three-dimensionally in principle. Modification of the PTV margin from 5 to 10 mm was allowed for the craniocaudal direction when no critical organs, such as the duodenum, were close to the edge of the PTV.

Dose–volume constraints were made for liver, lung, and GI tract according to previous reports and to our own preliminary studies. The maximum tolerable dose (MTD) to the liver adopted in this study was 30 Gy, using a 2-Gy daily dose for total liver volume (12). The biologic effective dose with an α/β ratio of 2 (BED_2) of the MTD was 60 Gy. The volume of liver that could receive 40 Gy in 20 fractions was assumed to be 30% of the whole liver in a dose–volume histogram. Alteration of dose fractionation was allowed to reduce the daily dose to the GI tract. The MTD of the GI tract was 40 Gy in 20 fractions, or BED_2 of 80 Gy. Based on these considerations, the total doses and fractionation schedules are listed in the study protocol as guidelines (Table 1). For example, if the tumor is >5 cm and the edge of the organ at risks is less than 1 cm, only 48 Gy in 8 fractions can be used. If the tumor is less than 3 cm and the edge of the GTV is 3 cm or more distant from the organ at risks, 20 Gy in one session or some other schedule can be used. This schema was developed to allow clinical staff members to select schedules based on the preliminary results of dose–volume statistics. Because of the insufficient data on the MTD, several dose schedules were allowed to be chosen.

Megavoltage X-rays (6, 10 MV) from a linear accelerator with five to seven single isocenter, non-coplanar ports were used. The dose was prescribed at the isocenter, giving 80% of the isocentric dose to cover PTV. A round, 2-mm gold marker was implanted near the tumor, within 3 cm from the isocenter of the GTV in principle. The reliability of the inserted marker as the GTV surrogate has already been reported (9). In short, the relationship between the gravity center of the liver and the marker was reproducible in the sequential CT examination for more than 1 month. Two sets of fluoroscopic cameras in the treatment room were used for the real-time recognition of the marker every 0.033 s during the delivery of the therapeutic beam. The therapeutic beam was gated to irradiate the tumor only when the marker was within 2.0 mm of the planned coordinates in lateral, anteroposterior, and craniocaudal directions.

The patients were followed up with a physical examination, blood collection, and either CT or magnetic resonance imaging every 3 months for 1 year and every 4–6 months thereafter by radiation oncologists with the help of hepatologists.

The Kaplan-Meier method was used to calculate the overall survival, local control, and intrahepatic control rates, in which any new lesions were counted as a failure. Adverse effects were scored according to National Cancer Institute Common Toxicity Criteria for Adverse Events, version 3.

RESULTS

From 2001 to 2004, 18 lesions of 15 patients were entered into this study. The patients were aged 54–73 years (median, 57 years). Hepatic function before radiotherapy was classified as Child class A, B, and C in 12, 3, and 0 patients, respectively. Five patients suffered from hepatitis B virus, 9 from hepatitis C virus, and 1 from alcoholic hepatitis. Tumors were located at the hepatic segments S1, S2, S6, S7, and S8 according to the Couinaud classification (13) in 3, 4, 3, 1, and 7 patients, respectively. The tumor diameter ranged from 15 to 52 mm (mean, 36 mm; standard deviation, 14 mm).

The reasons for RTRT were as follows: too close to the portal vein or inferior vena cava for other treatments, such as RFA or PEI, in 4 patients; located at the hepatic dome (S8) and far from other treatments in 3 patients; residual disease after other treatment in 2 patients; and coexisting illness in 3 patients.

The prescribed doses and fractionation used in the actual study are shown in Table 1. Various schedules were used according to the size and position of the tumor to restrict the dose to the critical organ. The most common dose in this study was 48 Gy in 8 fractions. The biologic effective dose with an α/β ratio of 10 (BED_{10}) was distributed from 39 to 106 Gy without consideration for cell proliferation. Seventeen lesions were treated with a BED_{10} of $\geq$50 Gy, and 16 lesions were treated with a BED_{10} of $\geq$60 Gy or more (median, 76.8 Gy).

With a mean follow-up period of 20 months (range, 3–57 months), the overall survival rate was 44% (standard error [SE] 14%) at 21 months after RTRT (Fig. 1). Rates of 1- and 2-year actuarial survival after RTRT were 79% and 44%, respectively. The local control rate within the CTV was 83% (SE 11%) at 30 months after RTRT. The intrahepatic control rate was 34% (SE 13%) at 10 months and 17% at 2 years after RTRT (Fig. 1). There were two local failures. One patient with a 20-mm tumor was treated with 48 Gy in 8 fractions in 2 weeks and relapsed at 8 months from the

Table 1. Doses and fractionations used in the intercepting radiotherapy

			Tumor size (GTV) (cm)			Distance from OAR (cm)†		
Dose (Gy)/fraction	*n*	BED_2/BED_{10} (Gy)*	<3	3–5	>5	<1	1–3	>3
20/1	1	220/60	1	—	—	—	—	1
48/4	1	336/106	—	1	—	—	—	1
40/4	3	240/80	1	1	1	—	1	2
48/8	7	192/76.8	1	5	1	1	4	2
40/8	2	140/60	—	2	—	—	2	—
40/16	1	90/50	—	1	—	—	1	—
Out of protocol	3	37/8, 30/10, 40/20+36/8	—	2	1	2	1	—

Abbreviations: GTV = gross tumor volume; OAR = organ at risk.
Tumor sizes and distances from the organ at risk of the patients treated are shown for each dose/fractionation schedule.
* Biologic equivalent dose, assuming an α/β ratio of 2 and 10 for BED_2 and BED_{10}, respectively.
† Minimum distance between the edge of clinical target volume and OAR.

margin of the tumor. The patient was treated by TAE afterward and survived for 21 months. The other patient, with a 15-mm tumor, was treated with 20 Gy in one session and relapsed at 10 months from the inside of the GTV. The latter was treated again with RTRT, and the tumor was controlled for 8 months thereafter. No other patients received transarterial chemoembolization or local ablation in combination with RTRT. In cases in which we allowed reirradiation for the relapsed tumor as a part of the treatment, the local control rate of the radiotherapy was 92% at 30 months. The 2- and 5-year actuarial survival rates after the initial treatment for HCC were 93% and 52%, respectively.

A symptomatic complication due to the insertion of the fiducial marker occurred in 1 patient, who experienced transient bile ductal bleeding and inflammation. An adverse reaction due to radiation was seen in 2 patients. A transient gastric ulcer in a patient with a 50-mm tumor adjacent to the stomach was salvaged by emergency endoscopic treatment (Grade 3 adverse effect), and the patient has been alive with no evidence of disease at 58 months. Radiation pneumonitis in a patient with a 45-mm tumor at the hepatic dome without the requirement of medication (Grade 1 adverse effect) was observed at 4 months after RTRT. No radiologic change was found in the follow-up CT taken at 20 months after RTRT.

There were no encephalopathy and ascites in the patients without tumor progression. Changes in transaminase levels after RTRT were available in 10 patients and are shown in Fig. 2. Several patients experienced increased transaminase at the subacute phase after RTRT transiently. There was no Grade 4 toxicity of liver function due to radiation, and there were two Grade 3 toxicities of transient elevation of aspartate amino transaminase (elevation at least 5 to 10 times the upper limit of normal).

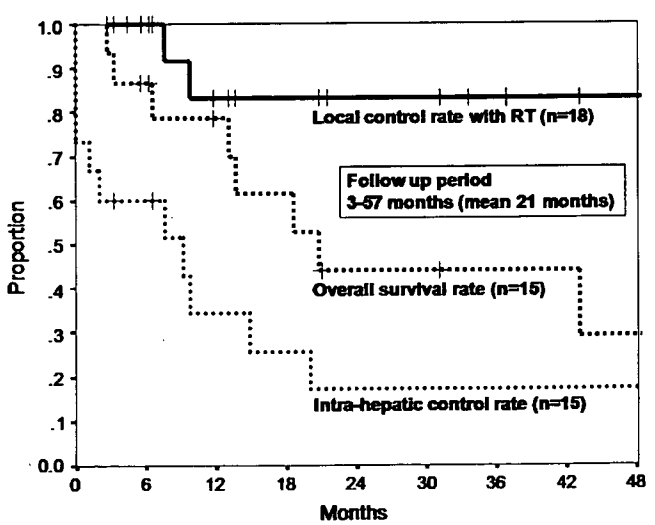

Fig. 1. Kaplan-Meier curves of overall survival and intrahepatic control rates for 15 patients with hepatocellular carcinoma (HCC) and local control rate with reirradiation for 18 HCC in the 15 patients. RT = radiotherapy.

DISCUSSION

Localized X-ray radiotherapy has been shown to achieve excellent local control rates with lower rates of radiation-induced liver dysfunction compared with conventional radiotherapy (4). Park *et al.* (14) reported a dose–response relationship in the local control rate of primary HCC. More recently, Park *et al.* (15) reported achieving an objective tumor response in 39 of 59 patients (66.1%), with complete response

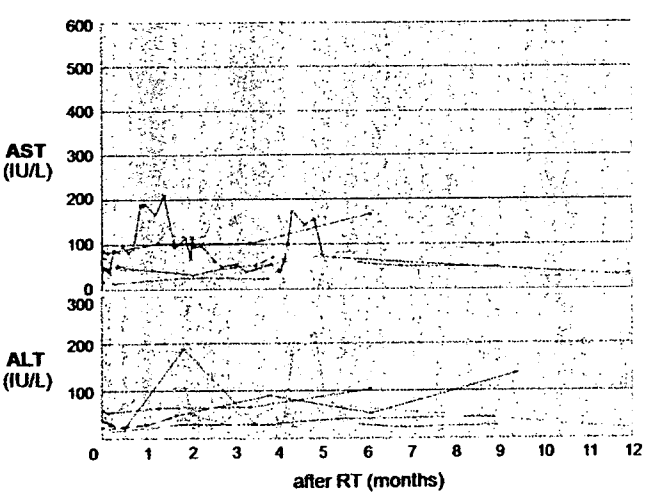

Fig. 2. Changes in transaminases. Alanine amino transaminase (ALT) and aspartate amino transaminase (AST) levels after real-time tumor-tracking radiotherapy (RT) in 10 patients.

in 5 patients and partial response in 34 patients using localized X-ray radiotherapy. The BED_{10} >50 Gy had a significantly better response rate (complete or partial response) of 72.8% compared with 46.7% with BED_{10} ≤50 Gy (p = 0.0299). The present study used BED_{10} >50 Gy in 17 of 18 lesions and showed local control rates of 83% after initial RTRT and 92% at 30 months when we included reirradiation with RTRT for the local relapse. Considering the smaller margin for CTV in RTRT compared with that in radiotherapy without a real-time tracking system, we can say that RTRT can accurately treat liver tumors in motion. The dose specification used in the present study was 80–90% at the periphery of the PTV. More accurate dose specification should be used in future studies.

Treatment of HCC by conventional radiotherapy is difficult owing to the adverse hepatic events that may be caused by radiation. Furuse *et al.* (3) observed Grade 3 toxicity in 18 of 46 patients (39.1%) with HCC within 3 months after radiotherapy of 50 Gy in 5 weeks, and Grade 4 toxicity in 11 of 33 patients (33.3%) thereafter, using an arrangement of two or three coplanar beams. Yang *et al.* (5) found hematologic toxicity in 34.6% and hepatobiliary complications in 26% of 153 patients with HCC treated with radiotherapy. Dawson *et al.* (16) carefully estimated the volume effect of the liver from more than 180 patients and found that RILD was not evident in patients with a mean liver dose of <31 Gy. They estimated that if <25% of the normal liver is treated with radiotherapy, then there may be no upper limit on the dose associated with RILD (17). In their estimation, the liver doses associated with a 5% risk of RILD for uniform irradiation of one third, two thirds, and the whole liver were 90, 47, and 39 Gy, respectively, with a daily dose of 2 Gy. This represents a much larger tolerance in the partial irradiation of the liver compared with whole-liver irradiation. We have seen transient elevation of serum transaminases after liver irradiation, but we have not seen any symptomatic RILD. This absence in our series confirms that the liver can tolerate high-dose partial volume irradiation.

Cheng *et al.* (18) found that HCC patients who were hepatitis B virus carriers or had Child-Pugh Class B cirrhosis presented with a significantly greater susceptibility to radiation-induced liver dysfunction after three-dimensional conformal radiotherapy. Considering that Asian patients with HCC usually suffered from viral hepatitis, dose distribution for the liver is crucial to the preservation of hepatic function. Dawson *et al.* (16) showed that the mean liver doses associated with a 5% risk of classic RILD for primary and metastatic liver cancer are 28 Gy and 32 Gy, respectively, at 2 Gy per fraction. Considering the lower dose tolerance of liver in patients with HCC, RTRT's benefit of reducing irradiation to the normal liver would be more apparent for primary HCC than for metastatic liver cancers.

It is well known that the GI tract is an important serial organ that is at risk in liver irradiation anatomically. In the recent literature, liver irradiation was not associated with serious adverse GI effects. Park *et al.* (14) reported a 5.1% complication rate of localized X-ray therapy for gastric or duodenal ulcer. Yang *et al.* (5) reported that out of 153 patients with HCC treated with radiotherapy, radiation-induced ulcers were found in the stomach (n = 9) and duodenum (n = 14), and bleeding was found in 11 patients (7%), including 1 case of fatal bleeding. We have experienced a single case (1 of 15; 6%) of Grade 3 but transient gastric ulcer; this rate was equivalent to that in the previous series. Yang *et al.* reported 35% hematologic toxicity and 2% pneumonitis. Considering the shorter treatment time and higher daily dose used in the present study, the equivalently low complication rate in our series may be attributable to the high-precision radiotherapy obtained by using RTRT.

Kawashima *et al.* (19) reported on proton treatment for 31 patients with HCC. During a median follow-up period of 31 months (range, 16–54 months), only 1 patient experienced recurrence of the primary tumor, and the 2-year actuarial local progression-free rate was 96% (95% confidence interval [CI] 88%–100%). The actuarial overall survival rate at 2 years was 66% (95% CI 48%–84%). Chiba *et al.* (6) of Tsukuba University reported on 192 HCCs in 162 patients treated with a proton beam at 72 Gy (range, 55–84 Gy) with a follow-up period of 32 months (range, 3–133 months) and found 86.9% local control and 23.5% overall survival at 5 years. Obviously, proton therapy is one of the best solutions using focal radiotherapy in dose distribution. Proton therapy using a real-time tumor-tracking system will become a radical treatment for HCC.

In conclusion, RTRT provided effective focal high doses to liver tumors adjacent to the critical organs or to tumors that are located too deep for other treatments. Because the fiducial markers for RTRT need not be implanted into the tumor itself, RTRT can be applied to HCC in patients who are not candidates for other surgical or nonsurgical treatments.

REFERENCES

1. Gannon CJ, Curley SA. The role of focal liver ablation in the treatment of unresectable primary and secondary malignant liver tumors. *Semin Radiat Oncol* 2005;15:265–272.
2. Liapi E, Hong K, Georgiades CS, *et al.* Three-dimensional rotational angiography: Introduction of an adjunctive tool for successful transarterial chemoembolization. *J Vasc Interv Radiol* 2005;16:1241–1245.
3. Furuse J, Ishii H, Nagase M, *et al.* Adverse hepatic events caused by radiotherapy for advanced hepatocellular carcinoma. *J Gastroenterol Hepatol* 2005;20:1512–1518.
4. Hawkins MA, Dawson LA. Radiation therapy for hepatocellular carcinoma: From palliation to cure. *Cancer* 2006;106:1653–1663.
5. Yang MH, Lee JH, Choi MS, *et al.* Gastrointestinal complications after radiation therapy in patients with hepatocellular carcinoma. *Hepatogastroenterology* 2005;52:1759–1763.
6. Chiba T, Tokuuye K, Matsuzaki Y, *et al.* Proton beam therapy for hepatocellular carcinoma: A retrospective review of 162 patients. *Clin Cancer Res* 2005;11:3799–3805.
7. Kato H, Tsujii H, Miyamoto T, *et al.* Results of the first prospective study of carbon ion radiotherapy for hepatocellular

carcinoma with liver cirrhosis. *Int J Radiat Oncol Biol Phys* 2004;59:1468–1476.
8. Shirato H, Shimizu S, Shimizu T, *et al.* Real-time tumor-tracking radiotherapy. *Lancet* 1999;353:1331–1332.
9. Kitamura K, Shirato H, Shimizu S, *et al.* Registration accuracy and possible migration of internal fiducial gold marker implanted in prostate and liver treated with real-time tumor-tracking radiation therapy (RTRT). *Radiother Oncol* 2002;62: 275–281.
10. Kitamura K, Shirato H, Seppenwoolde Y, *et al.* Tumor location, cirrhosis, and surgical history contribute to tumor movement in the liver, as measured during stereotactic irradiation using a real-time tumor-tracking radiotherapy system. *Int J Radiat Oncol Biol Phys* 2003;56:221–228.
11. Llovet JM, Bru C, Bruix J. Prognosis of hepatocellular carcinoma: The BCLC staging classification. *Semin Liver Dis* 1999;19:329–338.
12. Emami B, Lyman J, Brown A, *et al.* Tolerance of normal tissue to therapeutic irradiation. *Int J Radiat Oncol Bio Phys* 1991;21: 109–122.
13. Couinaud C. Le foie: Études anatomiques et chirurgicales. Paris: Masson; 1957. p. 9–12.
14. Park HC, Seong J, Han KH, *et al.* Dose-response relationship in local radiotherapy for hepatocellular carcinoma. *Int J Radiat Oncol Biol Phys* 2002;54:150–155.
15. Park W, Lim do H, Paik SW, *et al.* Local radiotherapy for patients with unresectable hepatocellular carcinoma. *Int J Radiat Oncol Biol Phys* 2005;61:1143–1150.
16. Dawson LA, Normolle D, Balter JM, *et al.* Analysis of radiation-induced liver disease using the Lyman NTCP model. *Int J Radiat Oncol Biol Phys* 2002;53:810–821.
17. Dawson LA, Ten Haken RK. Partial volume tolerance of the liver to radiation. *Semin Radiat Oncol* 2005;15:279–283.
18. Cheng JC, Wu JK, Lee PC, *et al.* Biologic susceptibility of hepatocellular carcinoma patients treated with radiotherapy to radiation-induced liver disease. *Int J Radiat Oncol Biol Phys* 2004;60:1502–1509.
19. Kawashima M, Furuse J, Nishio T, *et al.* Phase II study of radiotherapy employing proton beam for hepatocellular carcinoma. *J Clin Oncol* 2005;23:1839–1846.

Int J Clin Oncol (2007) 12:8–16
DOI 10.1007/s10147-006-0633-y

REVIEW ARTICLE

Hiroki Shirato · Shinichi Shimizu · Kei Kitamura
Rikiya Onimaru

Organ motion in image-guided radiotherapy: lessons from real-time tumor-tracking radiotherapy

Received: October 31, 2006

Abstract External radiotherapy using imaging technology for patient setup is often called image-guided radiotherapy (IGRT). The most important problem to solve in IGRT is organ motion. Four-dimensional radiotherapy (4DRT), in which the accuracy of localization is improved – not only in space but also in time – in comparison to 3DRT, is required in IGRT. Real-time tumor-tracking radiotherapy (RTRT) has been shown to be feasible for performing 4DRT with the aid of a fiducial marker near the tumor. Lung, liver, prostate, spinal/paraspinal, gynecological, head and neck, esophagus, and pancreas tumors are now ready for dose escalation studies using RTRT.

Key words Image-guided radiotherapy · Real-time tumor-tracking radiotherapy · Gated radiotherapy · Intercepting radiotherapy · Pursuing radiotherapy · Four-dimensional radiotherapy

Introduction

In external radiotherapy, the precise localization of the target volume is the key issue. The development of diagnostic imaging modalities such as computed tomography (CT) and magnetic resonance imaging (MRI) has enabled the performance of three-dimensional conformal radiotherapy (3DCRT) and intensity-modulated radiotherapy (IMRT). For the radiosurgery of intracranial disease, rigid fixation of the skull has been successful in improving the registration of the virtual space during treatment planning in relation to the real space during the actual treatment.[1] For extracranial disease, imaging technology was introduced to guide patient setup in the treatment room.[2] External radiotherapy using imaging technology for patient setup is often called image-guided radiotherapy (IGRT).

H. Shirato (✉) · S. Shimizu · K. Kitamura · R. Onimaru
Division of Radiation Oncology, Department of Radiology, Hokkaido University School of Medicine, North-15 West-7, Kita-ku, 060-8638 Sapporo, Japan
Fax +81-11-706-7876
e-mail: hshirato@radi.med.hokudai.ac.jp

The most important problem in IGRT is organ motion. Organ motion should be taken into account in any IGRT for extracranial diseases. In other words, accuracy in time as well as space is required in IGRT. Four-dimensional radiotherapy (4DRT) is IGRT in which the localization accuracy – not only in space but also in time – is improved in comparison to that in 3DRT. By definition, 4DRT is best performed with a sophisticated IGRT system by which the tumor position is monitored during the delivery of the therapeutic beam. Jiang[3] in a review, pointed out that there is only one system which can monitor the internal position of a tumor during irradiation: the real-time tumor-tracking radiotherapy (RTRT) system developed at Hokkaido University Hospital and made by Mitsubishi Electronics (Tokyo, Japan). As there are already many reviews of IGRT elsewhere, we concentrate in this article on a review of RTRT.

The Japanese Society of Therapeutic Radiology and Oncology (JASTRO) has defined RTRT as external radiotherapy which utilizes real-time tracking technology during the delivery of irradiation. There are two types of RTRT in principle (Fig. 1). One is intercepting irradiation, in which the therapeutic beam is delivered only when the tumor is within the gating window. The other is pursuing irradiation, in which the therapeutic beam is continuously delivered pursuing the position of the tumor. The following review deals with intercepting irradiation for which research started in 1996 at Hokkaido University Hospital.[4]

Lung

Three-dimensional (3D) treatment planning has often been performed while patients breathe freely, with the assumption that the CT images represent the average position of the tumor. Shimizu et al.[5] have investigated the impact of respiratory movement on the free-breathing CT images of small lung tumors using sequential CT scanning with the same table position. Using a preparatory free-breathing CT scan, the patient's couch was fixed at the position where

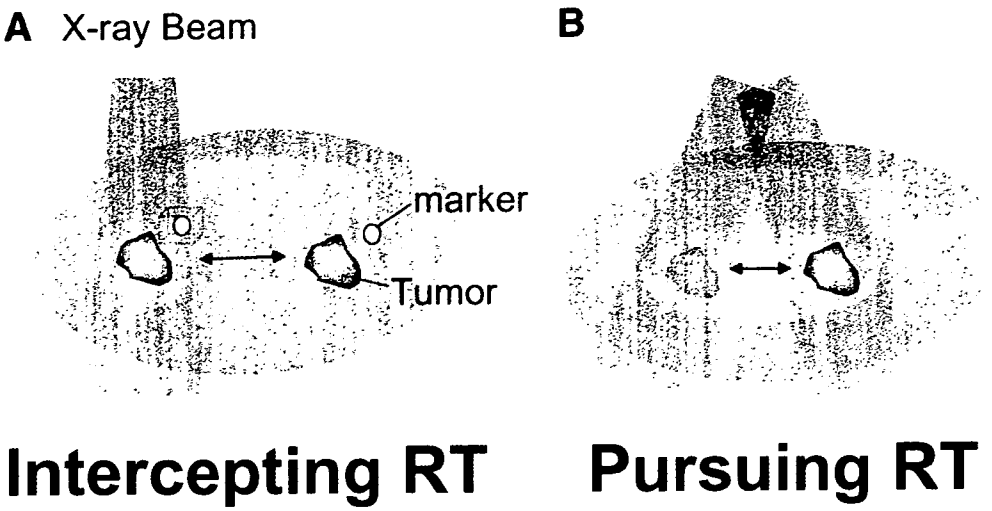

Fig. 1A,B. Two types of real-time tumor-tracking radiotherapy (RTRT). **A** Intercepting irradiation; **B** pursuing irradiation

each tumor showed its maximum diameter on the image. For 16 tumors, over 20 sequential CT images were taken every 2s, with a 1-s acquisition time occurring during free breathing. For each tumor, the distance between the surface of the CT table and the posterior border of the tumor was measured, to determine whether the edge of the tumor was sufficiently included in the planning target volume (PTV) during normal breathing. In the sequential CT scanning, the tumor itself was not visible in the examination slice in 21% (75/357) of cases. There were statistically significant differences between lower-lobe tumors (39.4%; 71/180) and upper-lobe tumors (0%; 0/89; $P < 0.01$) and between lower-lobe tumors and middle-lobe tumors (8.9%; 4/45; $P < 0.01$) in the incidence of the disappearance of the tumor from the image. The mean difference between the maximum and minimum distances between the surface of the CT table and the posterior border of the tumor was 6.4mm (range, 2.1–24.4mm). They concluded that 3D treatment planning for lung carcinoma, without considering organ motion, would significantly underdose many lesions, especially those in the lower lobe.

To achieve precise 3D conformal radiotherapy for mobile tumors, a new radiotherapy system and its treatment planning system were developed and used for clinical practice. Shirato et al.[6] developed a linear accelerator synchronized with a fluoroscopic RTRT system with which the 3D coordinates of a 2.0-mm gold marker in the tumor could be determined every 0.03s. The 3D relationships between the marker and the tumor at different respiratory phases are evaluated using a CT image at each respiratory phase, whereby the optimum phase can be selected to synchronize with irradiation (4D treatment planning). The linear accelerator is triggered to irradiate the tumor only when the marker is located within the region of the planned coordinates relative to the isocenter. The coordinates of the marker were detected with an accuracy of ±1mm during radiotherapy in the phantom experiment. The time delay between recognition of the marker position and the start or stop of megavoltage X-ray irradiation was 0.03s.

The RTRT system consists of four sets of diagnostic X-ray television systems (two of which offer an unobstructed view of the patient at any time), an image processor unit, a gating control unit, and an image display unit.[7] The system recognizes the position of a 2.0-mm gold marker in the human body 30 times per s, using two X-ray television systems. The marker is inserted in or near the tumor, using image-guided implantation. The accuracy of the system and the additional dose due to the diagnostic X-ray were examined in a phantom, and the geometric performance of the system was evaluated in four patients. The phantom experiment demonstrated that the geometric accuracy of the tumor-tracking system was better than 1.5mm for moving targets up to a speed of 40mm/s. The dose due to the diagnostic X-ray monitoring ranged from 0.01% to 1% of the target dose for a 2.0-Gy irradiation of a chest phantom. Shimizu et al.[7] concluded that the RTRT system significantly improved the accuracy of irradiation of targets in motion at the expense of an acceptable amount of diagnostic X-ray exposure.

The RTRT system was useful to analyze the movement of an internal marker. Shimizu et al.[8] investigated the 3D movement of lung tumors through an inserted internal marker, using the RTRT system, and evaluated the efficacy of this system in reducing the internal margin. Four patients with lung cancer were analyzed. A 2.0-mm gold marker was inserted into the tumor. The RTRT system triggered the linear accelerator to irradiate the tumor only when the marker was located within the predetermined "permitted dislocation" of ±1 to ±3mm according to the patient's characteristics. They analyzed 10413–14893 data sets for each of the four patients. The range of marker movement during normal breathing (beam-off period) was compared with that during gated irradiation (beam-on period) by Student's *t*-test. The range of marker movement during the beam-off period was 5.5–10.0mm in the right-left (RL) direction, 6.8–15.9mm in the craniocaudal (CC) direction, and 8.1–14.6mm in the anteroposterior (AP) direction. The range during the beam-on period was reduced to within 5.3mm in

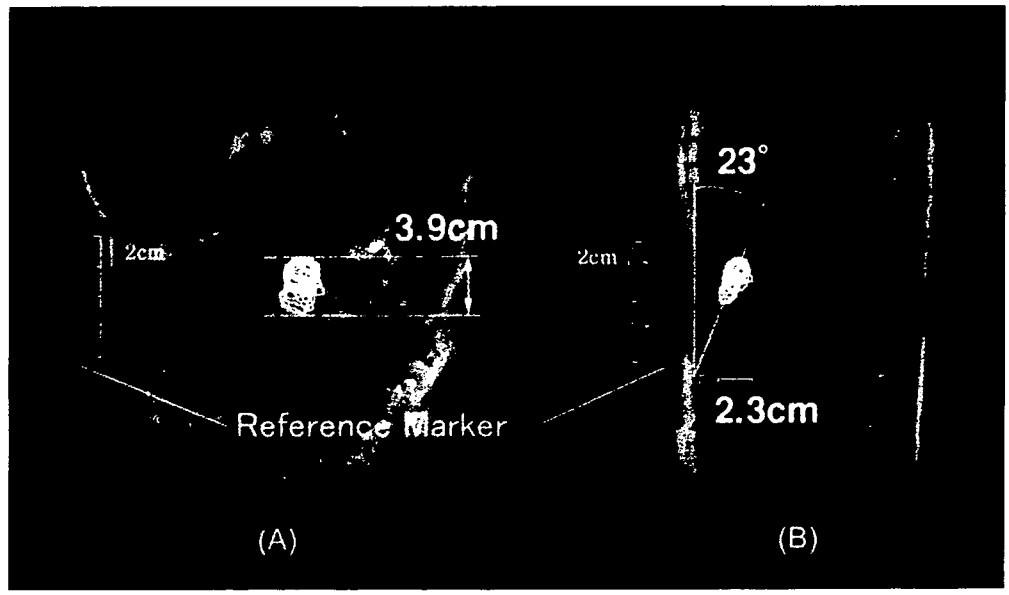

Fig. 2A,B. Four-dimensional (4D) treatment planning, using dynamic magnetic resonance imaging (MRI), for liver cancers. This patient had a liver tumor which had an amplitude of 3.9 cm in the craniocaudal (CC) direction and 2.3 cm in the anteroposterior (AP) direction on dynamic MRI. The internal target volume can be determined by using the summation of sequential images during several respiratory cycles. (From reference 11, with permission)

all directions in all four patients. A significant difference was found between the mean of the range during the beam-off period and the mean of the range during the beam-on period in the RL ($P = 0.007$), CC ($P = 0.025$), and AP ($P = 0.002$) coordinates, respectively. The results of Shimizu et al.[8] showed that treatment with megavoltage X-rays was properly given when the tumor marker moved into the "permitted dislocation" zone from the planned position.

In 2002, Seppenwoolde et al.[9] performed a precise analysis of the behavior of tumor motion in lung tissue to model tumor movement, using the data of 20 patients treated with the RTRT system at Hokkaido University Hospital. The recorded tumor motion was analyzed in terms of the amplitude and curvature of the tumor motion in three directions, the differences in breathing level during treatment, hysteresis (the difference between the inhalation and exhalation trajectory of the tumor), and the amplitude of tumor motion induced by cardiac motion. They confirmed that the average amplitude of the tumor motion was greatest (12 ± 2 mm [SD]) in the CC direction for tumors situated in the lower lobes and not attached to rigid structures such as the chest wall or vertebrae. For the RL and AP directions, tumor motion was small for both upper- and lower-lobe tumors (2 ± 1 mm). The time-averaged tumor position was closer to the exhale position, because the tumor spent more time in the exhalation than in the inhalation phase. The tumor motion was modeled as a sinusoidal movement with varying asymmetry. The tumor position in the exhale phase was more stable than the tumor position in the inhale phase during individual treatment fields. However, in many patients, shifts in the exhale tumor position were observed intra- and interfractionally. These shifts were the result of patient relaxation, gravity (posterior direction), setup errors, and/or patient movement. The 3D trajectory of the tumor showed hysteresis, which ranged from 1 to 5 mm, for 10 of the 21 tumors. The extent of hysteresis and the amplitude of the tumor motion remained fairly constant during the entire treatment. Changes in shape of the trajectory of the tumor were observed between subsequent treatment days for only 1 patient. Fourier analysis revealed that for 7 of the 21 tumors, measurable motion in the range of 1 to 4 mm was caused by the cardiac beat. These tumors were located near the heart or were attached to the aortic arch. The motion due to the heartbeat was greatest in the RL direction. Seppenwoolde et al.[9] suggested that tumor motion due to hysteresis and heartbeat could lower treatment efficiency in gated treatments or could lead to a geographic miss in conventional or active-breathing controlled treatments.

In another study using RTRT, 20 lung tumors in 18 patients were given high-dose hypofractionated focal irradiation (35–48 Gy in 4–8 fractions in 4–10 days) with a planning target volume margin of 5 mm for the tumor.[10] On the whole, 13 (65%) of the 20 tumors were successfully treated with RTRT. Local tumor control was achieved and maintained for all 12 patients (13 tumors) who were treated with RTRT, with a median follow-up of 9 months (range, 5–15 months). Localized radiation pneumonitis was found radiographically in the lung volume that was irradiated with about 20 Gy, and was without symptoms in all but 1 patient. The excellent initial response and low incidence of clinical complications suggest that high-dose hypofractionated focal irradiation, using the RTRT system, could be a good local treatment for peripheral-type lung tumors.

Liver

Four-dimensional (4D) treatment planning using dynamic 3D images was first reported by Shimizu et al.,[11] using not CT but magnetic resonance imaging (MRI; Fig. 2). They investigated the 3D movement of a spherical liver tumor during respiration with MRI, using a high-speed sequence. A marker was placed on the surface of the patient as a distance reference. Repetition time (TR) was 7.7 ms, echo time